COGNITIVE NEUROSCIENCE

Sequential effects in reaching reveal efficient coding in motor planning

Tianhe Wang[1,2]*, Yifan Fang[1], David Whitney[1,2,3]

The nervous system uses prior information to enhance movement accuracy, yet the underlying computational mechanisms remain relatively unclear. Prevailing motor control models emphasize Bayesian inference, where prior information is integrated to optimally estimate the current state. An alternative framework, efficient coding, proposes that the system dynamically reallocates encoding resources on the basis of environmental statistics—a mechanism highlighted in perception while underappreciated in motor control. We compared these frameworks in reaching movements, focusing on how the system leverages short-term priors in unpredictable environments. Unexpectedly, sequential effects aligned with the efficient coding model and contradicted Bayesian models. Specifically, current movements were biased in the opposite direction of previous movements, and movement variability decreased when successive reaches were similar. We further explored the temporal dynamics of these effects and showed that sequential bias is enhanced by intrinsic motor variability. These findings, accompanied by model comparisons, further support efficient coding in motor planning.

INTRODUCTION

Our experiences shape how we perceive and interact with the world. For instance, when facing ambiguous visual stimuli, humans are more likely to identify familiar objects than novel ones (*1*, *2*). Similarly, in reaching tasks, participants infer the state of the environment on the basis of previous observations to apply an optimal action (*3*–*5*). Those processes have been formalized with Bayesian observer models (*2*, *3*, *6*, *7*), which posit that the system maintains an internal prior on the basis of past observations and integrates this prior knowledge with new sensory input to form optimal estimates (*8*). This integration reduces variability in estimation, thereby increasing the overall response accuracy.

The Bayesian framework has substantially influenced theories of motor control and motor learning (*3*, *5*, *9*, *10*). For example, when localizing hand position, agents combine information from different sensory inputs in a Bayesian-optimal way (*9*, *11*, *12*). Moreover, sensorimotor learning theories posit that the system uses error information to update the sensorimotor map on the basis of a Bayes rule (*13*, *14*). Furthermore, Bayesian principles have been applied to interpret history effects in reaching tasks. Previous research has shown that after repeatedly performing one action, future movements would be biased toward the repeated direction—a phenomenon known as use-dependent learning (*15*, *16*). The Bayesian model explains this phenomenon by positing that the integration of previous motor goals with the current goal induces a behavioral bias toward the prior mean (Fig. 1, A and B) (*17*).

While Bayesian models have been extensively tested in motor control, these tasks often share two key characteristics that may limit the generalizability of those findings. First, the targets used in previous studies frequently have strong statistical structures, making it easy for participants to anticipate future movements (*18*). For example, many studies have sampled targets from unimodal distributions (*15*, *17*, *19*), allowing participants to predict the mean movement direction. Even in center-out reaching tasks, most experiments have used only a very small number of targets (*20*–*23*), thereby confining the possible motor plans to a very limited subspace. Second, those studies examined effects on the basis of a stable representation of the prior, which is estimated from many observations and remains constant over time.

However, contrary to those two prerequisites, in many real-life situations, motor goals can change rapidly across time in a relatively unpredictable way (*18*, *24*). For example, a basketball player needs to constantly change their motor plans in real time—suddenly shifting direction, accelerating, jumping, or making quick passes—in response to the unpredictable actions of opponents and teammates. Similarly, when shopping for groceries, the location of each item on the shelf varies, so reaching for one product is independent of where the next one might be. In these cases, the motor system must plan each movement independently rather than relying on a consistent prior. It remains unclear whether Bayesian mechanisms would be beneficial in such volatile environments. Alternatively, other computational mechanisms might be applied when motor goals vary on a short timescale.

An alternative framework, known as efficient coding, offers a distinct perspective on how the brain is constrained by environmental statistics (*25*–*28*). Efficient coding posits that the nervous system minimizes redundancy by maximizing the mutual information that can be carried by the limited resources (Fig. 1C) (*29*–*32*). In the perceptual domain, it refers to a strategy to encode information in the most compact and effective manner (*25*, *26*). In motor control, efficient coding can be taken as a way to avoid redundancy in the control system and maximize the overall accuracy. For example, rather than controlling each muscle individually, the brain might coordinate groups of muscles into synergies or modules (*33*, *34*).

While both the efficient coding model and Bayesian framework use prior information in a computationally optimal manner, the former is an adaptive mechanism applied to the encoding process, while the latter emphasizes how the brain decodes information on the basis of experience. As the main goal of the motor system is to encode a movement plan, the efficient coding principles might actually be more relevant (*23*). Previous theoretical work (*29*, *30*) suggested that efficient coding will induce biases in the opposite direction of the prior mean (Fig. 1D), a prediction opposite to the Bayesian model. While these signatures of efficient coding have been extensively studied in perceptual systems (*25*, *29*, *35*, *36*), it is less clear whether they apply to motor planning.

[1]Department of Psychology, University of California, Berkeley, Berkeley, CA, USA. [2]Department of Neuroscience, University of California, Berkeley, Berkeley, CA, USA. [3]Vision Science Program, University of California, Berkeley, Berkeley, CA, USA. *Corresponding author. Email: tianhewang@berkeley.edu

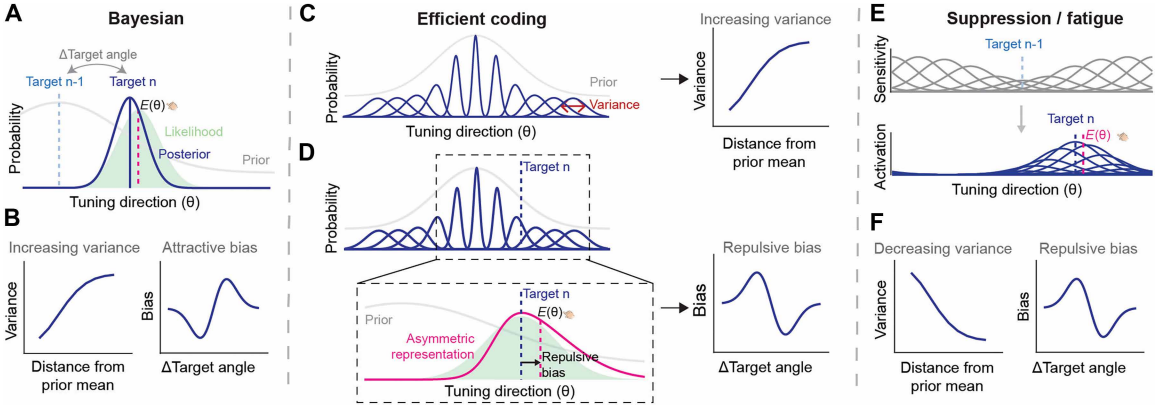

Fig. 1. Models for sequential effects in motor planning. (**A**) Illustration of a Bayesian model in motor planning. (**B**) The Bayesian model predicts increasing variance and attractive bias. (**C**) Schematic of an efficient coding framework. The motor system distributes encoding resources such that precision across different directions matches the prior distribution (gray). The family of blue curves (channels) shows encoding functions for different movement directions, with their variability constrained by the prior; the encoding variance increases as the current target diverges from the prior mean (right). (**D**) Imagine that a target appears on the right side of the prior mean. We show a zoomed-in view of the representation function (pink curve) for this target. Given that the width of the channels varies across tuning directions, the population response is asymmetric compared to the Gaussian encoding function in the absence of efficient coding (green-shaded region). Specifically, encoding variability is reduced on the left side and increased on the right side, creating a flatter tail extending away from the prior mean. As a result, the mean of this asymmetric representation function (pink dash line), which represents the movement direction ($E[\theta]$), is shifted rightward. Right: If we assume that the prior is determined by the movement direction in the previous trial, the efficient coding model predicts a repulsive sequential bias. (**E**) Illustration of the suppression model. The sensitivity of the unit tuned to the previous movement decreases, which causes an asymmetric representation of the subsequent movement direction. (**F**) The suppression model predicts decreasing variance and repulsive bias.

To understand how motor planning is adjusted on the basis of prior information in volatile environments, we aim to examine sequential effects in a center-out reaching task where the target is randomly sampled from a uniform circular distribution. As such, no mean movement direction can be predicted, and each movement is completely independent. While the overall prior is not informative in this situation, the system may maintain a short-term prior that is updated quickly when the goals change rapidly (*37*, *38*). This flexibility could be particularly beneficial for the motor system, which may need to repeat similar movements in quick succession, although not necessarily over extended periods.

Following the Bayesian model, prior updating would generate an attractive sequential effect, where the current response is biased toward previous responses that have just been performed (Fig. 1, A and B) (*17*, *37*, *38*). This effect, known as serial dependence, has been widely observed in perceptual tasks across different modalities (*39*–*42*). On the other hand, the efficient coding models predict that the current movement will be biased away from the previous movement. As such, efficient coding and Bayesian integration generate opposite predictions on the sequential effect, allowing us to distinguish between these two theoretical frameworks in the current study. In addition, we explored the temporal dynamics of these sequential effects and how they are modulated by intrinsic motor variability, which helps further differentiate between the models. The empirical and computational results together illustrate how the motor planning system adapts to the statistical properties in a dynamic environment.

RESULTS

Repulsive sequential bias in reaching

To examine motor sequential effects in an unpredictable environment, in Experiment (Exp) 1, we used an online reaching experiment where participants control a cursor with a trackpad. In each trial, a target appeared at a random position along an invisible circle and participants made a center-out reaching movement from a central start position toward the target (Fig. 2, A and B). The cursor was invisible during the movement to prevent online corrections. Endpoint feedback was provided after the movement to indicate the hand position at the target radius.

To obtain an accurate assessment of the sequential effect, we eliminated the impact of systematic bias by fitting a motor bias function based on the target position (Fig. 2C) for each participant. The residual error, representing the deviation from this fitted motor bias function, was defined as deviation (*37*, *38*, *43*, *44*) and was used to analyze the sequential effects.

We observed a repulsive sequential bias in reaching when movement deviation is plotted as a function of the angular difference between the current and previous targets (ΔTarget). We found that the direction of movement in the current trial (trial N) was biased away from the previous target (trial N-1; Fig. 2D), with the magnitude of this repulsive effect increasing with ΔTarget, peaking at 1.5° for a ΔTarget of ~60°. This bias function aligns with predictions from the efficient coding model rather than the Bayesian model. To quantify the size of the sequential bias, we calculated a sequential effect index (SE index), defined as the difference between the average bias for ΔTarget from −90° to 0° and 0° to 90°. A positive SE index signified a repulsive effect. We found an SE index significantly larger than 0 in trial N-1 [$t(25) = 9.5$, $P < 0.001$, $d = 1.9$] and trial N-2 [$t(25) = 2.8$, $P = 0.010$, $d = 0.55$] but not in trial N-3 [$t(25) = -0.10$, $P = 0.92$, $d = -0.02$; Fig. 2E], occurring ~6 s earlier. However, when we replicated Exp 1 with longer intertrial intervals (ITIs), we found that the strength of the sequential effect only showed a moderate decrease with a 6-s interval (Fig. 3, A and B; also see Supplementary Result 1). As such, the attenuation of the sequential effect depended on both the passing time and intervening information.

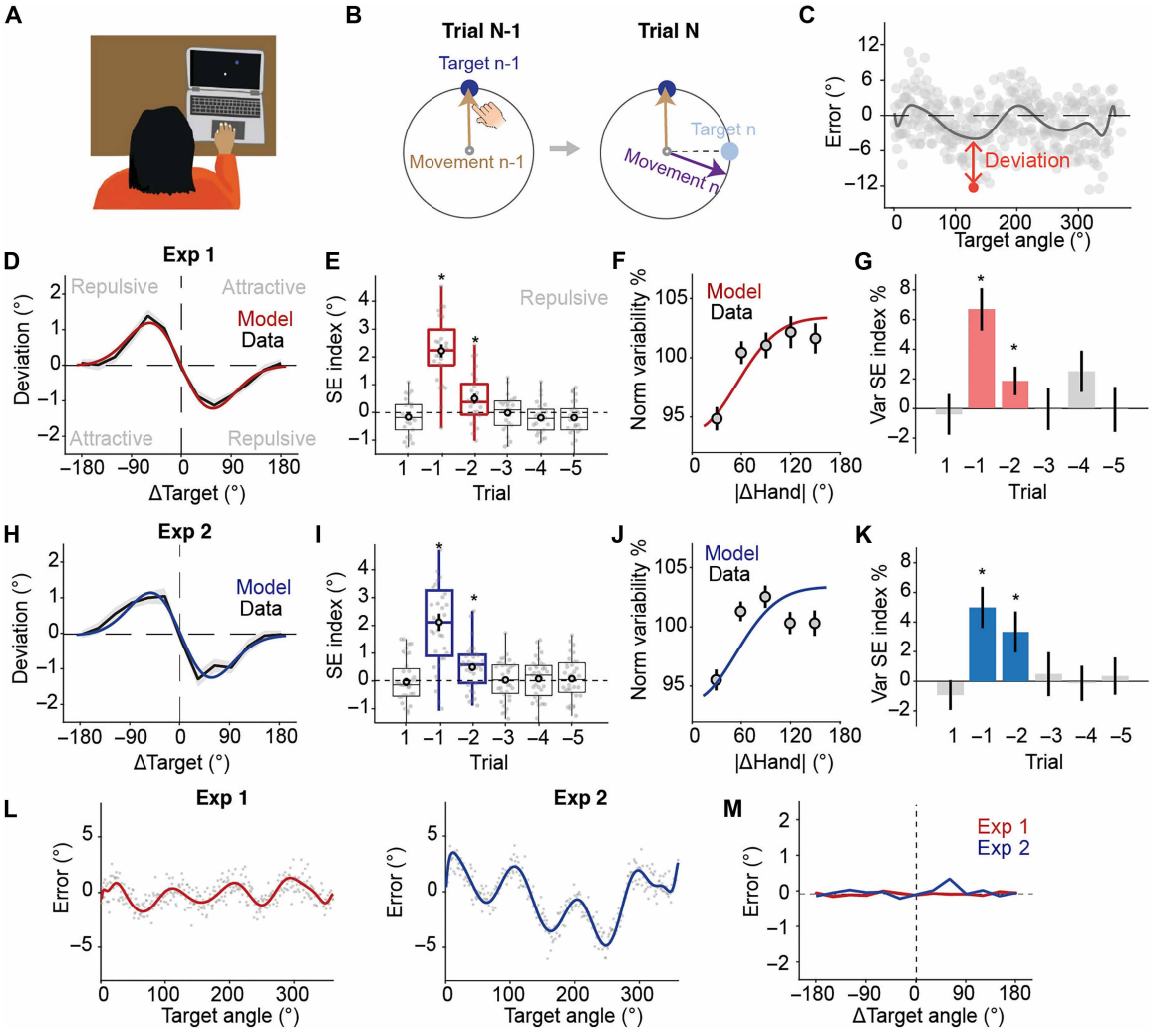

Fig. 2. Sequential effects in reaching. (**A**) Task setup for Exp 1 to Exp 4. Participants made center-out reaching movements using a trackpad. Visual stimuli of target and cursor were present on the laptop monitor. (**B**) Illustration of the repulsive bias predicted by the efficient coding model. (**C**) Reaching errors of a sample participant. The error is composed of two components: systematic motor bias relative to target position and "deviation," defined as the difference between the current response and the bias. The gray curve shows the smoothed motor bias function. (**D**) Sequential bias in Exp 1: The motor deviation of trial N was plotted as a function of the difference in the target angle between trial N and trial N-1 (ΔTarget). This figure shows a repulsive sequential effect. (**E**) SE index showing the influence of the target in trial N+1 and trials N-1 to N-5 on the direction of reaching in trial N. (**F**) The normalized movement variance increased with the distance between movement N and movement N-1 (|ΔHand|). (**G**) SE index derived from a general linear model between normalized movement variance and |ΔHand| for trial N+1 and trials N-1 to N-5. (**H** to **K**). Sequential effects in Exp 2. The only difference between Exp 1 and Exp 2 was the lack of feedback in Exp 2. Results were very similar to panels (D) to (G). (**L**) Systematic motor bias in Exp 1 and Exp 2. Dots indicate the group-averaged reaching angle to a target. The thick line represents a smoothed function. (**M**) As a control analysis, the systematic motor bias itself generates no sequential effects. Error bars and shaded areas in (D) to (K) indicate the standard error (applied to all figures). *$P < 0.02$.

Sequential effects in reaching align with the efficient coding model

The repulsive sequential biases observed in Exp 1 support the predictions of the efficient coding model rather than the Bayesian model. However, we note that an alternative explanation for this effect could be suppressive modulation or fatigue in the units tuned to the recently performed movement direction. The suppression model predicts repulsive sequential bias as a result of the asymmetric responses of units on the suppressed and unsuppressed sides (Fig. 1E). However, unlike the efficient coding and Bayesian models, which both facilitate the processing of repeated stimuli, the suppression model posits that movements closer to the previous movement are encoded with less precision and exhibit greater variability compared to those further away (Fig. 1F).

To compare the efficient coding model and suppression model, we measured the sequential effect as a function of movement variance. Consistent with the efficient coding model, the movement variance increased with the distance between the directions of two consecutive movements (Fig. 2F). As such, the repulsive sequential bias is unlikely to be due to fatigue. We quantified this effect by fitting a sigmoid function with motor variance as the dependent variable and the difference in hand angle as the independent variable, pooling data from all participants. The SE index was defined as the amplitude of the sigmoid predicted by the best-fit function (Fig. 2F).

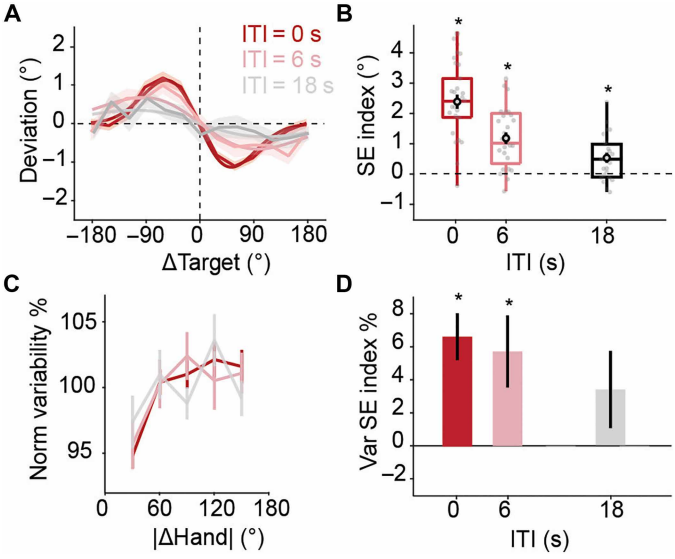

Fig. 3. Temporal dynamics of the sequential effects in reaching. (**A**) Sequential effect in the movement direction for three ITI conditions. The thinner lines indicate the data, and the thicker lines indicate the prediction of the efficient coding model. (**B**) SE index with different ITI conditions. Different from what has been observed under the three-back condition in Exp 1 (which had a ~6-s delay), the SE index was significant under the 6- and 18-s ITI conditions, indicating that the effect decreased with both time and trial number. Error bars and shaded areas indicate the standard error. (**C** and **D**) Sequential effects in motor variance were modulated by the ITI. A significant SE index was found under the 6-s ITI condition. *$P < 0.02$.

Similar to the sequential bias, this SE index of movement variance dropped rapidly across trials: A significant effect was found for only trial N-1 ($P < 0.001$) and N-2 ($P = 0.026$; Fig. 2G), as measured by bootstrap resampling. The effect disappeared for trial N-3 ($P = 0.98$), which occurred ~6 s earlier. The sequential effect in movement variance confirms that while there was a repulsive bias, the motor system uses previous information to increase the overall accuracy in reaching, consistent with the key idea of the efficient coding model.

We note that a potential issue in Exp 1 is that endpoint feedback could facilitate the recalibration of the sensorimotor system. This recalibration process might be specific to areas near the recently reached positions, potentially contributing to the observed sequential effect in motor variance. To eliminate the potential influence of sensorimotor recalibration, we conducted a replication of Exp 1 without endpoint feedback (Exp 2). The results showed remarkably similar sequential effects in both movement bias and variance (Fig. 2, H to K), confirming that these effects were independent of visual feedback or sensorimotor recalibration.

Dissociating sequential effects in movement and perception

Sequential effects have been widely observed in perceptual tasks (*39*, *40*, *45*). While we tried to minimize the role of visual uncertainty and perceptual working memory in Exp 1, a more rigorous examination was necessary to differentiate effects originating in the motor versus the perceptual systems (*46*). To this end, in Exp 3, we implemented a design where participants were instructed to either move directly toward the target (Standard condition, 75% of trials) or in the opposite direction (Opposite condition, 25% of trials). As a critical test of the source of these sequential effects in Exp 1, we analyzed scenarios where trial N-1 was an Opposite trial and trial N was a Standard trial (Fig. 4A, bottom). In such cases, the inconsistency between the movement direction and the target in trial N allowed us to disentangle the influences of target location representation from the motor control itself. If the repulsive bias was primarily driven by motor factors, the direction in trial N would be repelled by the movement in trial N-1. Conversely, if the perception of the target location was the cause, trial N's reaching direction would be repelled by the perceived location of the target in trial N-1.

When two consecutive trials were both Standard trials (Fig. 4A, top), we observed a repulsive bias similar to that in Exp 1 (Fig. 4B). Crucially, when trial N-1 was an Opposite trial and trial N was a Standard trial, the direction in trial N was repelled away by the previous reaching movement [$t(40) = 4.4$, $P < 0.001$, $d = 0.68$], not by the previous target location (Fig. 4C). The magnitude of this repulsive effect from the previous movement was comparable to that observed when both trials N and N-1 were Standard conditions, indicated by the SE indexes [$t(40) = 0.70$, $P = 0.49$, $d = 0.11$; Fig. 4D]. Moreover, when examining the sequential effect on motor variance, we found that the variance increased with the difference in hand angle ($P < 0.001$, bootstrap; Fig. 4E) rather than the difference in target angle ($P = 0.20$; Fig. 4, F and G). These results suggested that the sequential effects in Exp 1 and Exp 2 were rooted in the motor system rather than the perceptual system.

We have shown that the sequential bias in Exp 1 to Exp 3 was caused by movement; however, it remains possible that this effect could be mediated by perception. For instance, the movement from trial N-1 might repulse the perception in trial N, thereby affecting the subsequent movement (mediated hypothesis). Alternatively, the current movement could be directly repelled away by the previous movement (direct hypothesis). To distinguish between these hypotheses, we examined cases where trial N-1 was a Standard trial and trial N was an Opposite trial (Fig. 4H). Under the mediated hypothesis, the current perception is repelled away from the previous movement, so we would expect the current movement to be attracted toward movement N-1 when participants are instructed to move in a direction opposite that of target N. In contrast, the direct hypothesis predicts the current movement to be repelled from the target/movement in trial N-1 (Fig. 4I). Our findings aligned with the direct hypothesis (Fig. 4, J and K). On the basis of the results from Exp 3, we concluded that the current movement was directly influenced by the previous movement.

While Exp 3 provides strong evidence that the repulsive effect resides in the motor system, a potential issue remains: The center-out reaching is always correlated with a return movement where participants move in the opposite direction to return to the center. In principle, the repulsive effect based on previous outward movement could be interpreted as an attraction toward the return movement. To control this possibility, in Exp 4, we reset the cursor to a random position on the target ring after outward reaching movement (Fig. 5A) and asked participants to bring this cursor back to the center. This manipulation fully decorrelated the outward reaching movement and returning movements in trial N-1 (Fig. 5B), allowing us to analyze their separate impacts on subsequent reaching movement. If the effects we observed in the original experiments were caused by an attractive effect from returning movement, then we anticipate observing attraction toward both previous returning movement and previous outward reaching movement when they are separately considered (Fig. 5C, middle). In contrast, if previous

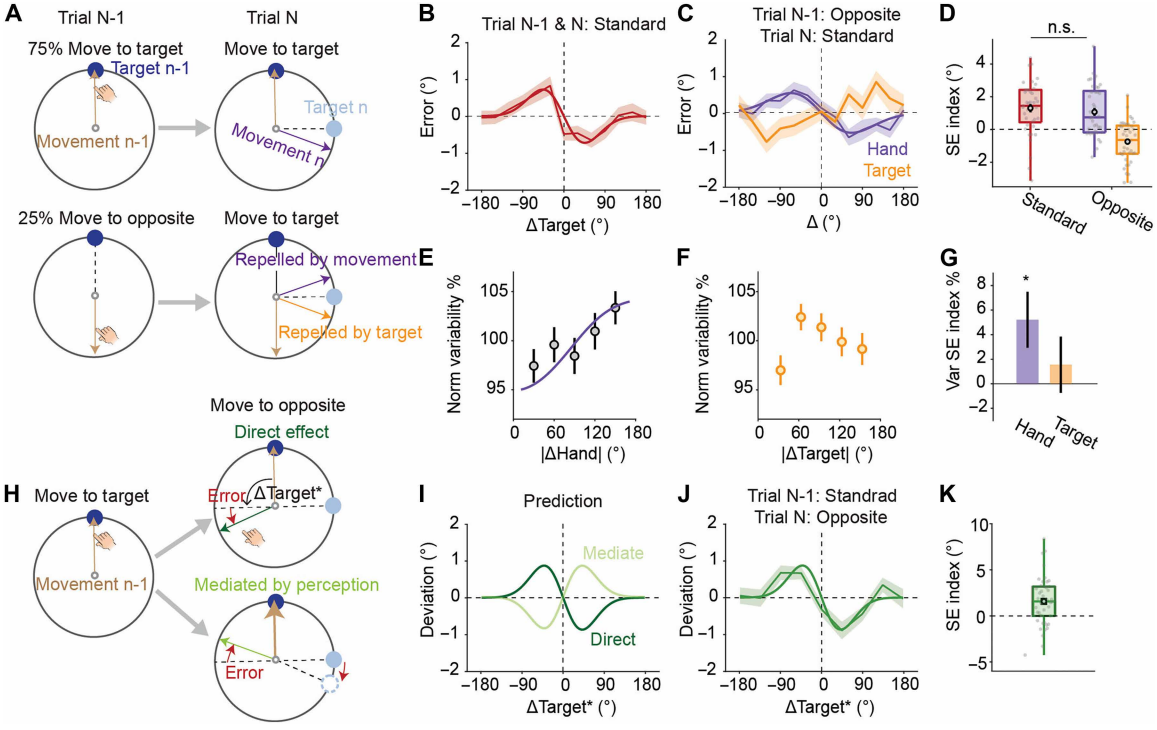

Fig. 4. Sequential effects in reaching were associated with motor movement rather than perception. (**A**) Design of Exp 3: In 75% of trials, participants moved toward the target (Standard), and in 25% of trials, they were directed to move in the opposite direction of the target (Opposite). A repulsive effect was expected when both trials N and N-1 were Standard trials (top row). In cases where trial N was a Standard trial and trial N-1 was an Opposite trial, the design allowed examination of whether the repulsive effect was triggered by target perception or movement (bottom row). (**B** and **C**) Sequential effect of motor bias when trial N-1 was a Standard trial (B) or an Opposite trial (C). Trial N was always a Standard trial. Thin lines indicate data; thick curves indicate the prediction of the efficient coding model. (**D**) The sequential bias was similar across (B) and (C) when the SE index after the Opposite trial was measured on the basis of ΔHand rather than ΔTarget. n.s., not significant. (**E** and **F**) After an Opposite trial, movement variance increased as a function of ΔHand (E) rather than ΔTarget (F). (**G**) Coefficients from the linear regression shown in (E) and (F). (**H**) To examine whether the effect was directly caused by the previous movement or was mediated by perception, we focused on the case where trial N was an Opposite trial and trial N-1 was a Standard trial. ΔTarget*: difference between the opposite position of the current target and the previous target. (**I**) Different predictions of the sequential bias following the direct and mediated hypotheses. (**J**) The sequential bias was consistent with the direct hypothesis. (**K**) The SE index indicates that the current movement was significantly repelled from the previous movement. *$P < 0.001$.

movements caused a repulsive effect, we would observe a bias function similar to what was observed in Exp 1 to Exp 3 (Fig. 5C, left).

Following the efficient coding model, we again observed a repulsive bias from the previous outward reaching movement [Fig. 5, D and E; $t(28) = 5.6$, $P < 0.001$, $d = 1.0$] when its direction was independent of the returning movement. We also observed that outward reaching movement was repulsed away by the returning movement [$t(28) = 2.7$, $P = 0.007$, $d = 0.54$], although this bias was much weaker than the effect from the previous outward reaching movement [Fig. 5E; $t(28) = 3.2$, $P = 0.003$, $d = 0.59$]. A similar sequential effect from the outward-reaching movement was also observed in motor variance ($P < 0.001$, bootstrap; Fig. 5, F and G), whereas the impact of the returning movements was not significant ($P = 0.98$, bootstrap). The weaker effect from the returning movement is expected, as the generalization of sequential effects may be context-dependent. Previous studies have indicated that the start position serves as a strong contextual cue for motor planning (*47*, *48*). Given that initial limb posture varies with the start position, generating the same movement vectors engages different neural activation patterns, thereby restricting generalization. As such, the change in start position between outward and inward reaching movements may result in a decreased influence of an inward movement on subsequent outward reaches.

Moreover, we note that the bias from the returning movement further demonstrates that the repulsive effect is not caused by visual attention, as participants had never attended to the opposite position of the reset cursor (Fig. 5A, dashed arrow). Together, these results together strongly support the idea that the current reaching is biased away from the previous reaching direction.

Encoding noise enhances repulsive sequential bias

Another key prediction of the efficient coding theory is that the sequential bias should be modulated by encoding noise. Specifically, increased noise within the system should lead to a broader distribution of the response signal. Consequently, the average response of the system will exhibit a larger repulsive bias relative to the prior mean (Fig. 6A). To examine this, we compared the sequential bias in reaching movements between the dominant hand and the nondominant hand, with the premise that encoding a movement with the nondominant hand incorporates more noise (Fig. 6B), which should increase the repulsive bias. In Exp 5, we performed a similar center-out reaching task, and participants were randomly instructed to use one hand per trial. To make sure that participants adhered to the instructions, we performed this experiment in a lab setup with the experimenter supervising the task (Fig. 6C). Participants moved

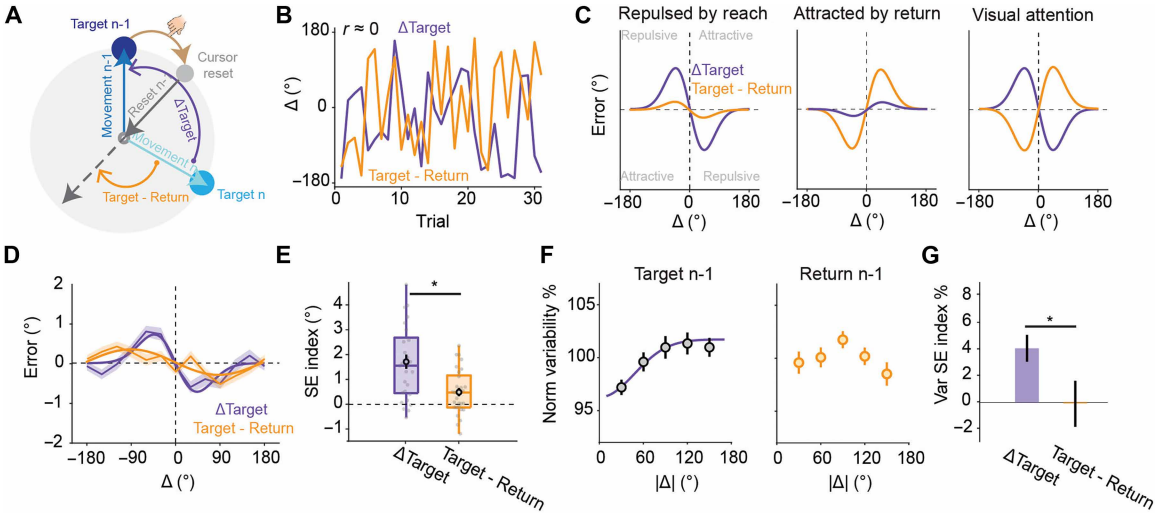

Fig. 5. Sequential effects in reaching are not due to the returning movement or visual attention. (**A**) Design of Exp 4. The cursor was reset to a random position on the target ring after each reach. Participants then moved the cursor to the start position before the next trial. (**B**) The difference between two successive targets (ΔTarget) and the difference between target n and the direction of the return movement (Target-Return) are independent. (**C**) Predictions of three possible hypotheses. Left: If the previous movement induces a repulsive effect on the current movement, we will observe repulsive effects from both the previous target and the returning movement. The effect of the latter might be smaller due to partial generalization across task configurations. Middle: If the repulsive effect from the previous outward-reaching movement in Exp 1 to Exp 3 was actually an attraction effect caused by the returning movement, we would observe attraction toward both the previous returning movement and previous outward-reaching movement when separated. Right: If the repulsive effect was caused by visual attention, we would observe a repulsive effect from the reset cursor position, which would translate into an attraction effect to the returning movement. (**D**) We observed repulsive effects for both the previous target and returning movement. The thin lines with shaded error bars indicate data, and the thick curve indicates the prediction of the efficient coding model. (**E**) The sequential bias was much stronger for ΔTarget compared to the returning movement. (**F**) The motor variance is modulated by the previous target position but not by the returning movement. (**G**) The coefficients of linear regression of motor variance are significantly larger for ΔTarget compared to the returning movement. *$P < 0.005$.

their occluded hand on a tablet, with the visual stimulus displayed on a monitor directly above (Fig. 6C). Consistent with our assumption, participants showed significantly lower motor variability with the dominant hand compared to the nondominant hand [$t(23) = 4.9$, $P < 0.001$, $d = 1.0$; Fig. 6D].

The results from Exp 5 provide compelling support for the efficient coding model. All main results were consistent with what we had observed in the online experiments. When we combined the data across the two hands, we observed a repulsive sequential bias [N-1: $t(23) = 4.7$, $P < 0.001$, $d = 0.96$; N-2: $t(23) = 2.6$, $P = 0.02$, $d = 0.55$; Fig. 6, E and F] and increased movement variance (N-1: $P < 0.001$, bootstrap, Fig. 6, G and H). We observed a larger sequential bias when the current movement was performed using the nondominant hand compared to the dominant hand [$t(23) = 4.7$, $P < 0.001$, $d = 0.97$; Fig. 6, I and J], supporting the prediction of the efficient coding theory that bias escalates with encoding noise in the motor system. We also observed a larger sequential bias when participants switched their hands (namely using different hands in trials N and N-1) compared to using the same hand [$t(23) = 6.7$, $P < 0.001$, $d = 1.4$; Fig. 6, K and L]. This effect is likely due to the dynamic allocation of encoding resources across hands, leading to increased encoding variability immediately after a hand switch and, consequently, a larger bias. Alternatively, more units might be recruited when repeating a movement with one hand, reducing the encoding noise as well as the sequential bias.

To further examine how the variability in the motor system influences the sequential bias, we analyzed the correlation between motor variance and the SE index in Exp 5. Consistent with the prediction of the efficient coding theory, we found a positive correlation between individual differences in variance and the SE index for both hands (Fig. 7A). A positive correlation was also found when we reexamined the data from Exp 1 and Exp 3 (Fig. 7, B and C). This correlation did not reach significance for Exp 2 and Exp 4 (fig. S1), but these two experiments showed much larger performance variance compared to the others, as feedback was omitted, so their power to detect the correlation was impaired; the measured correlations fell within the range expected given the higher performance variance (fig. S1D). Together, the results further supported the hypothesis that motor planning follows the principles of efficient coding.

Last, we also observed a priming effect in reaction time (RT). Consistent with the notion of efficient coding, RTs were shorter when the current target was close to the previous target for all experiments (fig. S2, A and B). Similarly, we also observed a movement time increase with the distance between successive targets in Exp 5 (fig. S3). This effect is much weaker compared to the RT, and we did not observe it for any online experiment, probably due to low temporal resolution for those setups. However, these RT and vigor effects may relate more to target detection than motor planning. For example, the RT for the current trial was influenced by targets presented in more than 10 trials in the past (fig. S2, C and D), which was very different from the temporal dynamics of sequential effects in movement direction or motor variance (Fig. 2, E and I). Moreover, in Exp 3, the RT priming effect was similar after both Opposite and Standard trials (fig. S2E), suggesting that the effect may be related to target detection rather than reaching, per se.

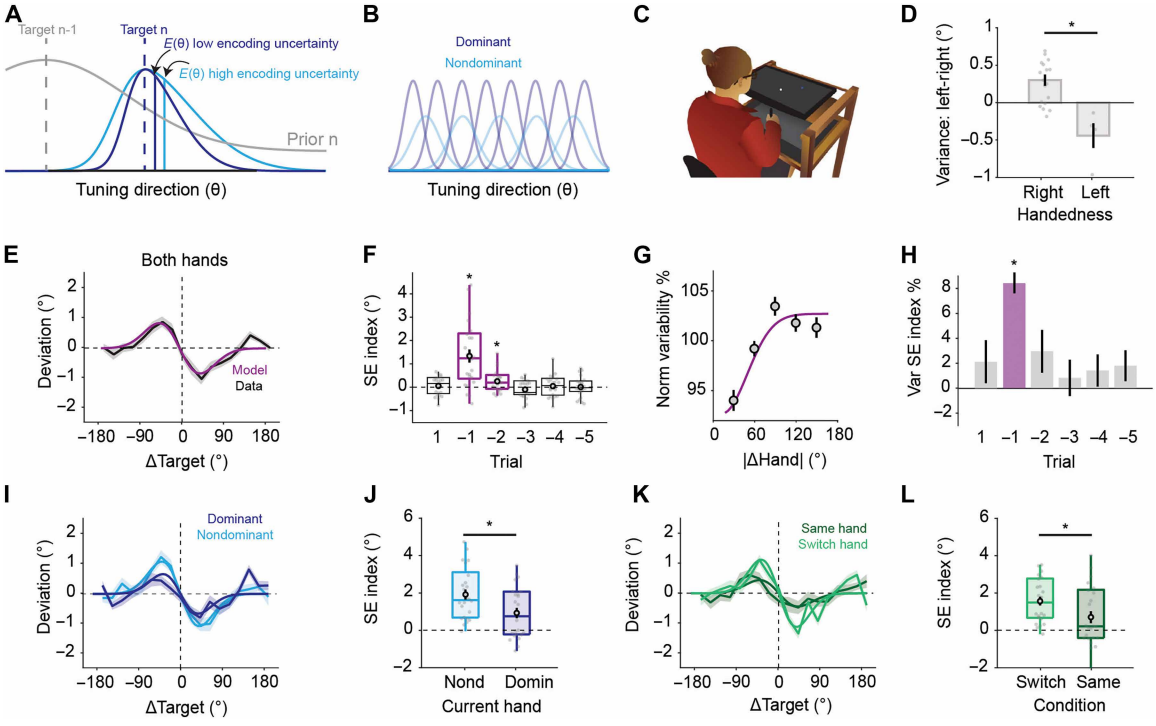

Fig. 6. The repulsive sequential bias increased with the encoding noise in the motor system. (**A**) Illustration of how encoding noise increases the repulsive bias on the basis of the efficient coding model. (**B**) We assumed that the nondominant hand has fewer movement planning units with higher encoding uncertainty, indicated by a broader tuning profile. (**C**) Illustration of the lab-based setup. (**D**) Difference in motor variance between the left and right hands. Right-handed participants showed nosier movements using their left hand and vice versa. (**E** and **F**) Sequential effect of motor bias (E) and the SE index (F) when data from both hands were collapsed. (**G** and **H**) Sequential effect of motor variance (G) and estimated coefficients from a general linear model (H). (**I** and **J**) A stronger repulsive bias was observed when the current movement was performed using the nondominant hand compared to the dominant hand. (**K** and **L**) A stronger repulsive bias was observed when participants switched hands compared to the situation when they used the same hand for trial N-1 and trial N. Error bars and shaded areas indicate the standard error. *$P < 0.001$.

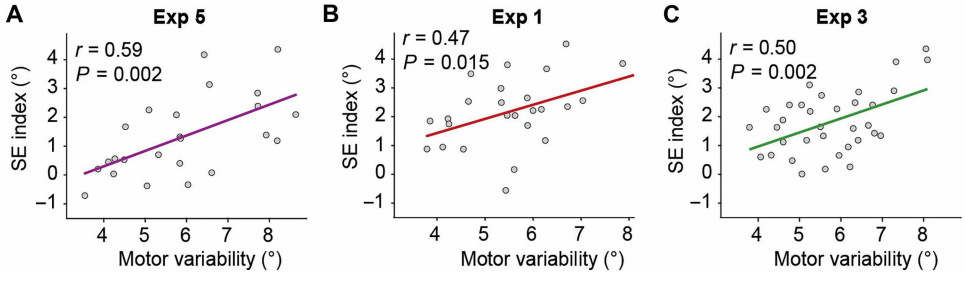

Fig. 7. The repulsive sequential bias increased with the motor variability across participants. Correlation between the SE index and the motor variance for Exp 5 (**A**), Exp 1 (**B**), and Exp 3 (**C**). Each dot is one participant. The colored line shows the best-fitted linear model. The *P* value was measured from the Pearson correlation.

DISCUSSION

The nervous system is dynamically tuned on the basis of past experiences to be optimally prepared for the current task. These adaptive processes induce sequential effects in behavior (*40*). In the present study, we examined the computational principles that govern the sequential effects in motor planning using reaching tasks with targets randomly sampled from a uniform circular distribution. Contrary to the prevailing belief that motor control is predominantly governed by Bayesian principles (*3*, *9*, *10*, *49*), we demonstrated a repulsive sequential bias in which the current movement is biased away from the direction of the previous movement. This anti-Bayesian behavior suggests that in less predictable environments, an alternative mechanism may also exist in motor control.

The sequential effects we observed indicate that motor planning follows the efficient coding model, a theory that posits that the nervous system maximizes mutual information by dynamically allocating resources to follow the prior distribution (*25*, *29*, *30*). Efficient coding has been widely applied to perceptual systems (*29*, *35*, *36*, *50*), and our results extend these principles to motor control. Our results confirm three key predictions of the efficient coding model in motor planning. First, the sequential bias was repulsive. Second, this effect was amplified when the reaching variance increased, as evidenced by differences between the left and right hands and the strong effect of individual differences in motor variability. Third, motor variance also exhibited a sequential effect, with movements closer to the previous one showing lower variability and higher accuracy. Together,

these sequential effects in reaching would not result from simple fatigue. Instead, they reflect an adaptive mechanism that enhances motor accuracy.

The temporal dynamics of the sequential effect highlight the flexibility of the motor system in adapting to environmental statistics. The repulsive effect diminished after only three trials (or ~30s based on Exp S1), suggesting that priors for efficient coding might be maintained by motor working memory (*51*). This adaptability is likely to be ideal for motor planning, given that one may need to repeat some quick actions, such as pressing a buzzer or knocking on a door. In contrast, it is less common for identical reaching movements to be necessary after a lapse of a minute. Consistent with this notion, in Exp 4, we found that the sequential effect decreased when participants consistently used one hand, as opposed to alternating between hands. This observation suggests that encoding resources can be preferentially allocated to the active hand when repeating the movement with the same hand, thereby increasing motor accuracy.

Sequential effects are well established in the visual system (*39*, *52*, *53*), but our results clearly distinguish current motor effects from the visual serial dependence reported in previous studies. First, the direction of the motor sequential bias observed in our study is opposite to the serial dependence typically seen in visual tasks (*39*, *43*, *45*, *53*). In our motor tasks, the current movement is repelled from the previous movement, whereas in visual perception tasks, the perceived target is usually attracted toward the previous target position (*43*). Second, when perception and movement are in opposite directions (Exp 4), sequential effects are determined by the movement direction rather than the target position (*45*). Third, our sequential effects are significantly modulated by handedness, further suggesting that they are associated with movement rather than perception.

The opposite directions of sequential biases in the motor and visual systems may reflect their distinct functional purposes and underlying mechanisms. In visual perception, the physical world is continuous and relatively stable (*54*–*56*), making it crucial for the visual system to maintain a consistent representation of the environment (*41*). Thus, using Bayesian decoding—which induces an attractive effect—is beneficial for visual perception, ensuring a coherent and reliable perception of the environment (*42*, *57*).

While the objects of perception in the world are physically stable, the actions we need to make upon these objects can change from moment to moment. The motor system, therefore, operates under distinct constraints. As motor goals can vary quickly over time (*20*), an attractive bias may not benefit motor planning in such dynamic contexts, whereas a decorrelation mechanism, such as efficient coding, may help to minimize repetitive errors and counteract attractive biases from other sources. A similar contrast between the stability and the flexibility of representation has been evident even within the visual system. For example, the perception of stable features like gender tends to show a stronger attractive serial dependence, whereas the more transient feature like the facial expression is likely to show a repulsive effect (*58*). In addition, Bayesian integration is typically associated with decoding processes that interpret sensory inputs on the basis of prior knowledge (*29*, *31*), whereas motor planning, at least by definition, is an encoding rather than decoding process, making Bayesian decoding mechanisms less applicable.

An open question remains whether the repulsive motor bias and the attractive biases induced by visual serial dependence may counterbalance each other. To isolate motor effects, we designed our study to minimize potential visual influences. For instance, visual effects are usually linked to perceptual uncertainty (*29*, *59*, *60*). A typical visual task for serial dependence usually features vague targets, brief presentations, or disappearance upon response. In contrast, our study used high-contrast targets that remained visible during movement. Future studies could use motor tasks with higher perceptual uncertainty, allowing both visual serial dependence and motor sequential effects to be observed. It is possible that the strengths of visual and motor effects are correlated and thus counteract each other.

The sequential effects in our study suggest that the motor planning system may implement efficient coding, adapting to environmental statistics by optimizing information transmission under resource constraints. While our model derives from ideal information-theoretic principles, prior work has proposed multiple biological implementations at the neural level. For example, lateral inhibition via anti-Hebbian plasticity can decorrelate input signals in the visual cortex, enhancing sensitivity to novel stimuli (*27*, *28*, *61*, *62*). Alternatively, later studies proposed that dynamically rescaled population responses can also increase perceptual sensitivity and reduce redundancy (*32*, *63*). Beyond sensory systems, efficient coding properties—emerging from optimally tuned neural populations—also explain reward prediction error encoding in decision-making circuits (*32*, *63*). Future studies could test whether similar mechanisms (e.g., decorrelation or optimal tuning) operate in motor regions to produce the observed repulsive biases.

The sequential bias identified in our study contrasts with a history-influenced effect known as use-dependent learning in motor control. Use-dependent learning refers to a bias toward repeated movements in the same direction (*15*, *16*, *64*), aligned with predictions of a Bayesian model. However, use-dependent learning only occurs for relatively predictable targets, whereas targets in our experiment were completely random. Moreover, the time course of use-dependent learning is very different from the repulsive sequential bias we observed. Use-dependent learning typically requires multiple trials to manifest (*15*, *19*, *22*), whereas the current repulsive effect emerges after a single trial. Last, use-dependent learning usually lasts for tens of trials, while the repulsive sequential effect reported here lasted for only two trials.

Our results suggest that the differing timescales of use-dependent learning and efficient coding may reflect a progressive shift of motor control strategy in developing a skilled movement. The repulsive bias induced by efficient coding could be beneficial in a volatile environment for several reasons, such as reducing repeated errors and enhancing sensitivity to changes in the environment, body, or target (*65*, *66*). However, there are instances where repeated, stable movement is desirable, such as when hammering a nail while holding it steady with one's fingers. Initially, efficient coding may increase the precision of movements. Those movements might be slow and performed with caution so that the system can correct undesired exploratory errors with online control. As the activity continues, use-dependent learning dominates to stabilize the movement, facilitating smooth and stable repetition without conscious control. Future studies should explore the intriguing possibility that there is a transition between efficient coding and use-dependent learning, which may reveal how the system balances the competing needs of flexibility and stability in motor planning.

MATERIALS AND METHODS

Participants

Testing was conducted online for Exp 1 to Exp 4 and in the lab for Exp 5. For the online studies, 183 young adults (86 females; age: 26.9 ± 4.8 years) were recruited using Prolific.io. Participants performed the experiment on their personal computers through a web-based platform for motor learning experiments. On the basis of a prescreening survey used by Prolific, all participants were right-handed and had normal or corrected-to-normal vision. These participants were paid $8/hour. For the lab-based experiments, we recruited 24 undergraduate students (15 females; mean age: 21.42 years; SD = 3.78 years) from the University of California, Berkeley community. Nineteen of the participants were right-handed and five were left-handed based on their scores on the Edinburgh handedness test (*67*); all had normal or corrected-to-normal vision. These participants were paid $20/hour. All experimental protocols were approved by the Institutional Review Board at the University of California, Berkeley (approval number: 2016-02-8439). Informed consent was obtained from all participants.

Design and procedure

Experiment 1

Exp 1 to Exp 3 were performed using our web-based experimental platform (*68*, *69*). The code was written in JavaScript and presented via Google Chrome, designed to run on any laptop computer. Visual stimuli were presented on the laptop monitor, and movements were produced on the trackpad. Data were collected and stored using Google Firebase.

Twenty-six participants (20 females) took part in Exp 1. To start each trial, participants moved the cursor to a white circle (radius: 1% of the screen height) positioned in the center of the screen. After 500 ms, a blue target circle (radius: 1% of the screen height) appeared with the radial distance set to 40% of the screen size. Target locations were randomly generated from 1° to 360° with a minimum step of 1°. The participant was instructed to produce a rapid shooting movement, attempting to move through the target. A feedback cursor (radius: 0.6% of screen height) appeared for 100 ms when the amplitude of the movement reached the target distance, indicating the angular position of the hand at that distance. The feedback cursor and target were then extinguished. If the movement time was >300 ms, the message "Too Slow" was presented on the screen for 500 ms. At the end of the trial, the position of the cursor was reset to a random position within a circle centered at the start position with a radius of 4% of the target distance. Participants moved the cursor back to the start position to initiate the next trial. Each participant completed 1080 trials in total.

To examine the temporal modulation of serial dependence, we performed two separate conditions where we extended the ITI to either 6 s (n = 28, 10 females) or 18 s (n = 23, 12 females) for two groups of participants, respectively. A message "wait" would be presented on the monitor between two trails. Participants were instructed to put their right hand on the trackpad and rest until they saw the message "move to center," which indicated the start of a new trial. Participants completed 880 (6-s condition) or 360 trials (18-s condition).

Experiment 2

To confirm that the effect observed in Exp 1 was not due to the existence of endpoint feedback, we replicated Exp 1 in Exp 2 without presenting any feedback after the movement. Other details of Exp 2 were identical to those of Exp 1. Thirty-six participants (21 females) took part in Exp 2.

Experiment 3

Exp 3 was designed to examine whether the sequential effect was induced by perception or movement. Forty-one participants (13 females) took part in Exp 4. The procedure of Exp 3 was essentially the same as in Exp 1. To evaluate whether this repulsive effect was perception-based or motor-based, we included trials (25%) in which the participants were instructed to move in the opposite direction of the target. Before each trial, an instruction message would appear on the screen to instruct participants to either "move to target" or "move to opposite." There were no consecutive "opposite" trails. Each participant completed 960 trials in total.

Experiment 4

Exp 4 was designed to isolate the effects of previous outward reaching and previous returning movements. Twenty-nine participants (10 females) took part in Exp 4. The procedure of Exp 4 was similar to that of Exp 2, with the difference that the cursor was reset to a random position on the target ring 1 s after the hand surpassed the target distance. Participants needed to bring the cursor back to the center position, which triggered the next trial.

Experiment 5

Exp 5 was designed to examine how motor variability influences the sequential reaching bias. Twenty-four participants (15 females; 19 right-handed and 5 left-handed) performed the experiment in the lab setup. Participants performed a center-out reaching task, holding a digitizing pen in the right or left hand to make horizontal movements on a digitizing tablet (49.3 cm by 32.7 cm; sampling rate, 100 Hz; Wacom, Vancouver, WA). The stimuli were displayed on a 120-Hz, 17-inch (43.18-cm) monitor (Planar Systems, Hillsboro, OR), which was mounted horizontally above the tablet (25 cm), to preclude the vision of the limb. The experiment was controlled by custom software coded in MATLAB (The MathWorks, Natick, MA), using Psychtoolbox extensions, and ran on a Dell OptiPlex 7040 computer (Dell, Round Rock, TX) with the Windows 7 operating system (Microsoft Co., Redmond, WA).

Participants made reaches from the center of the workspace to targets positioned at a radial distance of 8 cm. The start position and target location were indicated by a white annulus (1.2-cm diameter) and a filled blue circle (1.6 cm), respectively. The vision of the hand was occluded by the monitor, and the lights were extinguished in the room to minimize the peripheral vision of the arm. Feedback, when provided, was in the form of a 4-mm white cursor that appeared on the computer monitor, aligned with the position of the digitizing pen.

To start each trial, a letter "R" or "L" would be presented within the start circle to inform the participant which hand to use on this trial. Participants used the instructed hand to hold the pen and put the other hand on the side. The experimenter supervised the whole experiment to make sure that the participant applied the correct hand. After maintaining the cursor within the start circle for 500 ms, a target appeared. The participant was instructed to make a rapid slicing movement through the target. Right after their movement amplitude reached 8 cm, a cursor would be presented at that position for 1 s, providing feedback on the accuracy of the movement (angular position with respect to the target). After this interval, the target and cursor were extinguished. Another letter appeared at the start position, and participants changed hands accordingly. To guide the participant back to the start position without providing angular

information about the hand position, a white ring appeared denoting the participant's radial distance from the start position. Once the participant moved within 2 cm of the start position, the ring was extinguished, and a veridical cursor appeared to allow the participant to move their hand to the start position. If the movement time was >300 ms, the audio "Too Slow" was played right after the reaching.

The required hand was pseudorandomized, so there were four left-hand and four right-hand trials within every eight trials. Target locations were randomized in a way that both hands would visit targets from 1° to 360° (with a step of 1°) within every 720 trials. The whole experiment included 2160 trials and took about 4 hours. However, we allowed participants to end the experiment on the basis of their convenience. Fourteen of 24 participants finished all trials; other participants finished 1000 to 2000 trials.

Data analysis

We calculated the error of hand angle as a difference between the hand position when it reached the target distance and the target position. A positive hand angle denoted that the hand position was more clockwise than the target at the target radius. Trials with a movement duration longer than 500 ms or an error larger than 60° were excluded from the analyses. For the web-based experiment, 1.5% of trials were removed. For the lab-based experiment, 0.4% of trials were removed.

To analyze the sequential effect in movement, we regressed out the influence of systematic bias. Specifically, we fitted a function between motor bias and target angle using a polynomial function with a maximal power of 10 for each participant. We then subtracted this motor bias function from the motor error. The residual error was defined as motor "deviation" and applied to analyze the sequential effect (*37*, *38*, *43*, *44*).

To analyze the sequential bias of the movement direction, we measured the function of how motor deviation changed as a function of the difference of target position between trial N-1 and trial N (defined as ΔTarget). A function that lies in quadrants II and IV will suggest that the movement error was in the opposite direction of the previous target. To quantify sequential bias, we introduced the SE index that takes the difference between the average error within −90° to 0° ΔTarget and the average error within 0° to 90° ΔTarget. A positive SE index means a repulsive sequential effect and vice versa.

To further examine how the variability in the motor system influences the sequential bias, we calculated the Pearson correlation between the motor variance and the SE index for Exp 1, Exp 3, and Exp 4 (only for trials after a standard trial). The motor variance was very large under the no-feedback condition of Exp 2 compared to all other experiments, likely because of the drifting sensorimotor map without visual calibration (*70*, *71*). As such, the motor variance in Exp 2 was not a good measurement of encoding variability.

To analyze the sequential effect in motor variance, we calculated the absolute difference between movement N-1 and movement N (|ΔHand|). We flipped the sign of the deviation if ΔHand was negative. Then, we calculated the variance of deviation within each bin of 30°. The variance was then normalized by the average variance for each participant. To examine the tendency of how variance changed as a function of |ΔHand|, we applied a general linear model

$$\text{variance} = a + \frac{b-a}{e^{-c|\Delta\text{Hand}|}} \quad (1)$$

where a, b, and c are the three free parameters. The SE index was defined as the change in the output of the function when |ΔHand| increases from 30° to 150°. To estimate the distribution of the SE index, we applied bootstrap resampling 1000 times.

To analyze the priming effect in the reaction direction, we normalized the RT by subtracting the average reaction of each participant. We then plotted a function of how the normalized RT changes as a function of |ΔTarget|. The RT SE index is the difference between the average-normalized RT within 180° to 90° |ΔTarget| and the average RT within 0° to 90° |ΔTarget|. Simple t tests were conducted to determine whether the SE indexes were significantly different from 0. We confirmed that the data met the assumptions of a Gaussian distribution and homoscedasticity for all tests. The significance level was set at $P < 0.05$ (two-tailed).

Model

Efficient coding model

We assumed that the motor system encodes a movement direction (m) on the basis of an observed target direction (θ) following the rule of efficient coding. This model is based on previous models of efficient coding in perception (*26*, *29*, *31*). A key assumption of the model is that the encoding system allocates its resources to maximize the mutual information $I[\theta,m]$ between input θ and output m. By imposing a constraint to bound the total coding resources of the system (*29*), this requires the Fisher information $J(\theta)$ to be matched to the stimulus prior distribution $[p(\theta)]$: $p(\theta) \propto J(\theta)$. As such, coding resources are allocated such that the most likely movement direction is coded with the highest accuracy.

We next calculated the likelihood functions of how the system responds to different target directions with constraints of the prior distribution. Technically, the likelihood functions can be computed by assuming a symmetric Gaussian noise structure in a space where the Fisher information is uniform (the motor space, $\widetilde{\theta}$) and then transforming those symmetric likelihood functions back to the target space (θ). To construct a motor space with uniform Fisher information on the basis of the prior distribution of θ, one defines a mapping F from the target space (θ) to the motor space ($\widetilde{\theta}$) following (*29*)

$$\widetilde{\theta} = F(\theta) = \int_0^{\theta} p(\chi)d\chi \quad (2)$$

Given an input θ, the output m is computed as follows (*26*). We first calculated the response value r, which would be of the form θ + ϵ, where ϵ represents an error as a result of the intrinsic encoding noise of the system. Note that ϵ follows an asymmetric distribution in the target space (Fig. 1B). Let $\widetilde{\epsilon}$ represent the transformation of ϵ to the motor space. Given that we were assuming that $\widetilde{\epsilon}$ has a symmetric Gaussian distribution, the response value in the motor space would be $\widetilde{r} = F(\theta) + \widetilde{\epsilon}$, where $\widetilde{\epsilon} \sim N(0, \sigma^2)$, which gives a response value in the target space of

$$r = F^{-1}[F(\theta) + \tilde{\epsilon}] \quad (3)$$

Next, we assumed that the system knows that its response r is noisy. Therefore, it generates a distribution of the form $r + \delta$, where δ follows the same distribution as ϵ. If $\widetilde{\delta}$ represents the transformation of δ to the motor space, this distribution will be of the form $F^{-1}(r+\delta)$, where $\widetilde{\delta} \sim N(0, \sigma^2)$. Last, the system returns the expected value of this distribution as the output m

$$m = E\left[F^{-1}\left(r+\tilde{\delta}\right); \tilde{\delta}\right] \quad (4)$$

where $E(X; z)$ means the expected X as z varies. We defined $\phi\left(\widetilde{\theta}\right) = F^{-1}\left(\widetilde{\theta}\right)$. In the small-noise limit, we can take a second-order Taylor expansion

$$F^{-1}[F(\theta)+\epsilon] \approx F^{-1}[F(\theta)]+\phi'[F(\theta)] \times(\epsilon+\delta)+(1/2)\phi''[F(\theta)]\times(\epsilon+\delta)^2 \quad (5)$$

Considering Eqs. 3 to 5 together, we have

$$m \approx \theta + \phi'[F(\theta)]\epsilon + \frac{1}{2}\phi''\left(\sigma^2+\epsilon^2\right) \quad (6)$$

To estimate the motor bias predicted by the model, we calculated the expected value of m ($\hat{m}$) when ϵ varies, which can be expressed as

$$\hat{m} = E\left(m;\widetilde{\epsilon}\right) \approx \theta + \phi''\sigma^2 \quad (7)$$

In addition, the variance of m across trials can be expressed as

$$\mathrm{var}(m) \approx \left(\phi'\sigma\right)^2 \quad (8)$$

Given that the sequential effect in movement is influenced principally by the last movement, we assumed that the prior of the motor planning system is a mix of a uniform distribution across the whole space and a Gaussian distribution centered at the last target direction (θ_{n-1})

$$p(\theta) \propto k * U(0, 360) + (1-k)N\left(\theta_{n-1}, \rho^2\right) \quad (9)$$

where k is a scale factor controlling the relative contribution of the two distributions; ρ indicates the width of influence from the previous trial. To simulate the bias and the variance predicted by this efficient coding model, we computed the numerical approximation of ϕ'' and ϕ' on the basis of this prior function using an incremental approach.

This model includes three free parameters: k and ρ, which determine the shape of the prior, and σ, which reflects the encoding noise. Given that many parameter sets can produce similar bias patterns but different variance functions, we fitted the model by constraining both the bias and variance functions. Specifically, we predicted the deviations using the model and calculated the mean squared error (MSE) between these predictions and the observed data across all trials and participants. In addition, we computed the variance function and calculated the MSE between the predicted function and the empirical group-level variance. We then minimized the sum of these two MSEs to determine the best-fitting parameters.

Repeated suppression model

We considered two alternative models to explain the sequential effects in motor planning. The first model is a repeated suppression model, which assumes that neurons tuned to a specific direction become less sensitive after repeating a similar movement. Those modulations can enhance the sensitivity to the changes in the environment or/and encourage exploration. Here, we applied a population coding model with a group of neurons with Gaussian-shaped tuning functions. For a target direction θ, the unit tuned to the i ($i \in [0, \pi]$) direction generates a response r_i as follows

$$r_i = \mathrm{Norm}(\theta, i, d) \quad (10)$$

where $\mathrm{Norm}(\theta, i, d)$ is the probability density function of a Gaussian distribution with a mean of i and a standard deviation of d. The output of the system is determined by summing the activation of all neurons

$$\mathbf{m} = \sum_i \mathrm{s}_i \mathrm{r}_i \mathbf{v}_i \quad (11)$$

where $\mathbf{v}_i$ is a vector representing the tuning direction of unit i, $\mathbf{m}$ is a vector pointing toward the movement direction, and s_i is the sensitivity of unit i. After a movement in trial n, s_i is updated on the basis of the strength of the activation in unit i

$$\mathrm{s}_i\ (n+1) = 1 - a r_i(n) \quad (12)$$

where $a \in [0, 1]$is the suppression rate. As such, units that response more to the target in trial n will be more suppressed in the next trial.

Bayesian decoding model

The second alternative model we applied is a classic Bayesian decoding model that uses the prior distribution of θ to improve performance (*3*, *72*, *73*). The system generates a response r on the basis of a target direction θ. Considering Gaussian encoding noise, the relationship between r and θ can be expressed as follows

$$p(r|\theta) = \mathrm{Norm}(\theta, \sigma) \quad (13)$$

The model assumes that the system uses both the prior and this likelihood function to form a posterior estimation following Bayesian rules

$$p(\theta|r) = \frac{p(\theta)p(r|\theta)}{p(r)} \quad (14)$$

where $p(r)$ is a constant, $p(\theta)$ is the prior, $p(r\,|\,\theta)$ is the likelihood, and $p(\theta|r)$ is the posterior. The output of the system (m) is the posterior mean. For the Bayesian model, we used the same prior distribution (see Eq. 9) as the efficient coding model.

Supplementary Materials

This PDF file includes:

Supplementary Text
Figs. S1 to S3

REFERENCES AND NOTES

1. M. Bar, Visual objects in context. *Nat. Rev. Neurosci.* **5**, 617–629 (2004).
2. D. Kersten, P. Mamassian, A. Yuille, Object perception as Bayesian inference. *Annu. Rev. Psychol.* **55**, 271–304 (2004).
3. K. P. Körding, D. M. Wolpert, Bayesian integration in sensorimotor learning. *Nature* **427**, 244–247 (2004).
4. K. P. Kording, J. B. Tenenbaum, R. Shadmehr, The dynamics of memory as a consequence of optimal adaptation to a changing body. *Nat. Neurosci.* **10**, 779–786 (2007).
5. J. B. Heald, M. Lengyel, D. M. Wolpert, Contextual inference in learning and memory. *Trends Cogn. Sci.* **27**, 43–64 (2022).
6. M. Miyazaki, D. Nozaki, Y. Nakajima, Testing Bayesian models of human coincidence timing. *J. Neurophysiol.* **94**, 395–399 (2005).
7. M. Miyazaki, S. Yamamoto, S. Uchida, S. Kitazawa, Bayesian calibration of simultaneity in tactile temporal order judgment. *Nat. Neurosci.* **9**, 875–877 (2006).
8. D. C. Knill, A. Pouget, The Bayesian brain: The role of uncertainty in neural coding and computation. *Trends Neurosci.* **27**, 712–719 (2004).
9. K. Wei, K. Körding, Relevance of error: What drives motor adaptation? *J. Neurophysiol.* **101**, 655–664 (2009).
10. D. W. Franklin, D. M. Wolpert, Computational mechanisms of sensorimotor control. *Neuron* **72**, 425–442 (2011).
11. Z. Zhang, H. Wang, T. Zhang, Z. Nie, K. Wei, Perceptual error based on Bayesian cue combination drives implicit motor adaptation. *Elife* **13**, RP94608 (2024).
12. C. Kayser, L. Shams, Multisensory causal inference in the brain. *PLoS Biol.* **13**, e1002075 (2015).
13. D. M. Wolpert, R. C. Miall, M. Kawato, Internal models in the cerebellum. *Trends Cogn. Sci.* **2**, 338–347 (1998).
14. D. M. Wolpert, J. R. Flanagan, Motor prediction. *Curr. Biol.* **11**, R729–R732 (2001).
15. J. Diedrichsen, O. White, D. Newman, N. Lally, Use-dependent and error-based learning of motor behaviors. *J. Neurosci.* **30**, 5159–5166 (2010).
16. C. M. Butefisch, B. C. Davis, S. P. Wise, L. Sawaki, L. Kopylev, J. Classen, L. G. Cohen, Mechanisms of use-dependent plasticity in the human motor cortex. *Proc. Natl. Acad. Sci. U.S.A.* **97**, 3661–3665 (2000).

17. T. Verstynen, P. N. Sabes, How each movement changes the next: An experimental and theoretical study of fast adaptive priors in reaching. *J. Neurosci.* **31**, 10050–10059 (2011).
18. A. L. Wong, A. M. Haith, J. W. Krakauer, Motor planning. *Neuroscientist* **21**, 385–398 (2015).
19. W. Marinovic, E. Poh, A. de Rugy, T. J. Carroll, Action history influences subsequent movement via two distinct processes. *Elife* **6**, e26713 (2017).
20. A. L. Wong, A. M. Haith, Motor planning flexibly optimizes performance under uncertainty about task goals. *Nat. Commun.* **8**, 14624 (2017).
21. L. Alhussein, M. A. Smith, Motor planning under uncertainty. *Elife* **10**, e67019 (2021).
22. J. S. Tsay, H. E. Kim, A. Saxena, D. E. Parvin, T. Verstynen, R. B. Ivry, Dissociable use-dependent processes for volitional goal-directed reaching. *Proc. Biol. Sci.* **289**, 20220415 (2022).
23. H. Deng, A. Haith, Use-dependent biases as optimal action under information bottleneck. arXiv:2407.17793 [q-bio.NC] (2024); https://doi.org/10.48550/arXiv.2407.17793.
24. D. A. Rosenbaum, *Human Motor Control* (Academic Press, ed. 2, 2009).
25. M. S. Lewicki, Efficient coding of natural sounds. *Nat. Neurosci.* **5**, 356–363 (2002).
26. R. Polanía, M. Woodford, C. C. Ruff, Efficient coding of subjective value. *Nat. Neurosci.* **22**, 134–142 (2019).
27. H. B. Barlow, P. Földiák, "Adaptation and decorrelation in the cortex" in *The Computing Neuron*, R. Durbin, C. Miall, G. Mitchison, Eds. (Addison-Wesley, 1989), pp. 54–72.
28. H. B. Barlow, "The biological role of neocortex" in *Information Processing in the Cortex* (Springer Berlin Heidelberg, 1992), pp. 53–80.
29. X.-X. Wei, A. A. Stocker, A Bayesian observer model constrained by efficient coding can explain "anti-Bayesian" percepts. *Nat. Neurosci.* **18**, 1509–1517 (2015).
30. M. Hahn, X.-X. Wei, A unifying theory explains seemingly contradictory biases in perceptual estimation. *Nat. Neurosci.* **27**, 793–804 (2024).
31. X.-X. Wei, A. A. Stocker, Lawful relation between perceptual bias and discriminability. *Proc. Natl. Acad. Sci. U.S.A.* **114**, 10244–10249 (2017).
32. K. Louie, P. W. Glimcher, Efficient coding and the neural representation of value. *Ann. N. Y. Acad. Sci.* **1251**, 13–32 (2012).
33. M. L. Latash, Motor synergies and the equilibrium-point hypothesis. *Motor Control* **14**, 294–322 (2010).
34. M. L. Latash, J. P. Scholz, G. Schöner, Toward a new theory of motor synergies. *Motor Control* **11**, 276–308 (2007).
35. V. L. Ming, L. L. Holt, Efficient coding in human auditory perception. *J. Acoust. Soc. Am.* **126**, 1312–1320 (2009).
36. D. Ganguli, E. P. Simoncelli, Efficient sensory encoding and Bayesian inference with heterogeneous neural populations. *Neural Comput.* **26**, 2103–2134 (2014).
37. T. Wang, Y. Luo, R. B. Ivry, J. S. Tsay, E. Pöppel, Y. Bao, A unitary mechanism underlies adaptation to both local and global environmental statistics in time perception. *PLoS Comput. Biol.* **19**, e1011116 (2023).
38. M. Fritsche, E. Spaak, F. P. de Lange, A Bayesian and efficient observer model explains concurrent attractive and repulsive history biases in visual perception. *Elife* **9**, e55389 (2020).
39. J. Fischer, D. Whitney, Serial dependence in visual perception. *Nat. Neurosci.* **17**, 738–743 (2014).
40. A. Kiyonaga, J. M. Scimeca, D. P. Bliss, D. Whitney, Serial dependence across perception, attention, and memory. *Trends Cogn. Sci.* **21**, 493–497 (2017).
41. G. M. Cicchini, K. Mikellidou, D. C. Burr, Serial dependence in perception. *Annu. Rev. Psychol.* **75**, 129–154 (2024).
42. M. Manassi, D. Whitney, Continuity fields enhance visual perception through positive serial dependence. *Nat. Rev. Psychol.* **3**, 352–366 (2024).
43. M. Manassi, A. Liberman, A. Kosovicheva, K. Zhang, D. Whitney, Serial dependence in position occurs at the time of perception. *Psychon. Bull. Rev.* **25**, 2245–2253 (2018).
44. D. Pascucci, G. Mancuso, E. Santandrea, C. Della Libera, G. Plomp, L. Chelazzi, Laws of concatenated perception: Vision goes for novelty, decisions for perseverance. *PLoS Biol.* **17**, e3000144 (2019).
45. M. Manassi, Y. Murai, D. Whitney, Serial dependence in visual perception: A meta-analysis and review. *J. Vis.* **23**, 18 (2023).
46. G. M. Cicchini, K. Mikellidou, D. Burr, Serial dependencies act directly on perception. *J. Vis.* **17**, 6 (2017).
47. P. Baraduc, D. M. Wolpert, Adaptation to a visuomotor shift depends on the starting posture. *J. Neurophysiol.* **88**, 973–981 (2002).
48. A. M. E. Sarwary, D. F. Stegeman, L. P. J. Selen, W. P. Medendorp, Generalization and transfer of contextual cues in motor learning. *J. Neurophysiol.* **114**, 1565–1576 (2015).
49. J. B. Heald, M. Lengyel, D. M. Wolpert, Contextual inference underlies the learning of sensorimotor repertoires. *Nature* **600**, 489–493 (2021).
50. K. A. May, L. Zhaoping, Efficient coding theory predicts a tilt aftereffect from viewing untilted patterns. *Curr. Biol.* **26**, 1571–1576 (2016).
51. H. Hillman, T. Botthof, A. D. Forrence, S. D. McDougle, Dissociable codes in motor working memory. *Psychol. Sci.* **35**, 150–161 (2024).
52. M. Manassi, D. Whitney, Illusion of visual stability through active perceptual serial dependence. *Sci. Adv.* **8**, eabk2480 (2022).
53. M. Fornaciai, J. Park, Attractive serial dependence in the absence of an explicit task. *Psychol. Sci.* **29**, 437–446 (2018).
54. M. Angelini, G. Santucci, "On visual stability and visual consistency for progressive visual analytics," in *Proceedings of the 12th International Joint Conference on Computer Vision, Imaging and Computer Graphics Theory and Applications* (SCITEPRESS - Science and Technology Publications, 2017); http://dx.doi.org/10.5220/0006269703350341.
55. F. Pazhoohi, Visual experience: Sensation, cognition and constancy. *Eur. J. Psychol.* **10**, 204–207 (2014).
56. W. Epstein, *Stability and Constancy in Visual Perception: Mechanisms and Processes (Wiley Series in Behavior)* (John Wiley & Sons, 1977).
57. G. M. Cicchini, K. Mikellidou, D. C. Burr, The functional role of serial dependence. *Proc. R. Soc. B.* **285**, 20181722 (2018).
58. J. Taubert, D. Alais, D. Burr, Different coding strategies for the perception of stable and changeable facial attributes. *Sci. Rep.* **6**, 32239 (2016).
59. G. K. Gallagher, C. P. Benton, Stimulus uncertainty predicts serial dependence in orientation judgements. *J. Vis.* **22**, 6 (2022).
60. D. P. Bliss, J. J. Sun, M. D'Esposito, Serial dependence is absent at the time of perception but increases in visual working memory. *Sci. Rep.* **7**, 14739 (12/2017).
61. P. Földiák, Forming sparse representations by local anti-Hebbian learning. *Biol. Cybern.* **64**, 165–170 (1990).
62. H. B. Barlow, Single units and sensation: A neuron doctrine for perceptual psychology? *Perception* **1**, 371–394 (1972).
63. H. H. Schütt, D. Kim, W. J. Ma, Reward prediction error neurons implement an efficient code for reward. *Nat. Neurosci.* **27**, 1333–1339 (2024).
64. J. Classen, J. Liepert, S. P. Wise, M. Hallett, L. G. Cohen, Rapid plasticity of human cortical movement representation induced by practice. *J. Neurophysiol.* **79**, 1117–1123 (1998).
65. S. Eckmann, L. Klimmasch, B. E. Shi, J. Triesch, Active efficient coding explains the development of binocular vision and its failure in amblyopia. *Proc. Natl. Acad. Sci. U.S.A.* **117**, 6156–6162 (2020).
66. K. C. Hayes, R. G. Marteniuk, "9 - Dimensions of motor task complexity" in *Motor Control*, G. E. Stelmach, Ed. (Academic Press, 1976), pp. 201–228.
67. R. C. Oldfield, The assessment and analysis of handedness: The Edinburgh inventory. *Neuropsychologia* **9**, 97–113 (1971).
68. J. S. Tsay, R. B. Ivry, A. Lee, G. Avraham, Moving outside the lab: The viability of conducting sensorimotor learning studies online. *Neurons Behav. Data Anal. Theory* **5**, 1–22 (2021).
69. T. Wang, G. Avraham, J. S. Tsay, T. Thummala, R. B. Ivry, Advanced feedback enhances sensorimotor adaptation. *Curr. Biol.* **34**, 1076–7085.e5 (2024).
70. J. B. J. Smeets, J. J. van den Dobbelsteen, D. D. J. de Grave, R. J. van Beers, E. Brenner, Sensory integration does not lead to sensory calibration. *Proc. Natl. Acad. Sci. U.S.A.* **103**, 18781–18786 (2006).
71. J. Wann, S. Ibrahim, Does limb proprioception drift? *Exp. Brain Res.* **91**, 162–166 (1992).
72. M. Jazayeri, M. N. Shadlen, Temporal context calibrates interval timing. *Nat. Neurosci.* **13**, 1020–1026 (2010).
73. W. J. Ma, Organizing probabilistic models of perception. *Trends Cogn. Sci.* **16**, 511–518 (2012).

Acknowledgments: We thank R. Ivry for helpful discussions. **Funding:** This work was supported by NIH R01CA236793 to D.W. **Author contributions:** Conceptualization: T.W., Y.F., and D.W. Methodology: T.W. and Y.F. Investigation: T.W. and Y.F. Visualization: T.W. and Y.F. Supervision: D.W. Writing—original draft: T.W. and Y.F. Writing—review and editing: T.W., Y.F., and D.W. **Competing interests:** The authors declare that they have no competing interests. **Data and materials availability:** All data needed to evaluate the conclusions in the paper are present in the paper and/or the Supplementary Materials. All data and code are available at https://doi.org/10.5281/zenodo.15633726.

Submitted 9 January 2025
Accepted 25 July 2025
Published 27 August 2025
10.1126/sciadv.adv6572